

Evaluation of the impact of vitrification on the actin cytoskeleton of in vitro matured ovine oocytes by means of Raman microspectroscopy

Luisa Bogliolo · Ombretta Murrone · Massimo Piccinini ·
Federica Ariu · Sergio Ledda · Sara Tilocca ·
David F. Albertini

Received: 19 August 2014 / Accepted: 5 November 2014 / Published online: 16 November 2014
© Springer Science+Business Media New York 2014

Abstract

Purpose Investigation of the changes induced by vitrification on the cortical F-actin of in vitro matured ovine oocytes by Raman microspectroscopy (RMS).

Methods Cumulus-oocyte complexes, recovered from the ovaries of slaughtered sheep, were matured in vitro and vitrified following the Minimum Essential Volume method using cryotops. The cortical region of metaphase II (MII) oocytes (1) exposed to vitrification solutions but not cryopreserved (CPA-exp), (2) vitrified/warmed (VITRI), and (3) untreated (CTR) was analyzed by RMS. A chemical map of one quadrant of single CPA-exp, VITRI and CTR oocytes was, also, performed. In order to identify the region of Raman spectra representative of the cortical F-actin modification, a group of in vitro matured oocytes were incubated with latrunculin-A (LATA), a specific F-actin destabilizing drug, and processed for RMS analysis. Thereafter, all the oocytes were stained with rhodamine phalloidin and evaluated by fluorescence confocal microscopy. Raman spectra of the oocytes were, statistically, analyzed using Principal Component Analysis (PCA).

Results The PCA score plots showed a marked discrimination between CTR oocytes and CPA-exp/ VITRI groups. The main differences, highlighted by PCA loadings, were referable to

proteins (1657, 1440 and 1300 cm^{-1}) and, as indicated by LATA experiments, also included the changes of the F-actin. Analysis by confocal microscopy revealed a clear alteration of the cortical F-actin of CPA-exp and VITRI oocytes confirming RMS results.

Conclusions Raman microspectroscopy may represent an alternative analytical tool for investigating the biochemical modification of the oocyte cortex, including the F-actin cytoskeleton, during vitrification of in vitro matured ovine oocytes.

Keywords Oocyte · Cryopreservation · Raman microspectroscopy · Actin · Sheep

Introduction

Oocyte cryopreservation is a rapidly developing technology with considerable potential in the field of reproductive biotechnologies, in both the animal and human [1, 2]. Among the available cryopreservation techniques, vitrification is considered an interesting perspective for the animal oocytes, appearing less traumatic than slow freezing [3]. Moreover, based on the current evidence, we can state that the vitrification of human oocytes is a standardized technique, and today it is widely adopted [4, 5]. However, a number of variables, including patient age, oocyte quality, cryoprotectants types/concentrations and various vitrification devices may affect the final outcomes [1, 2, 5].

A component of the oocyte that can be damaged by the vitrification/warming procedure is the cytoskeleton [6–8]. The cytoskeleton network of the oocyte has a peculiar arrangement of microtubules, microfilaments and intermediate filaments and plays an important role during the maturation and the fertilization of the oocyte as well as in the early embryonic development [9, 10]. Several studies have shown that the

Capsule Raman microspectroscopy can be used to detect modification of the oocyte cortex following vitrification.

L. Bogliolo (✉) · O. Murrone · F. Ariu · S. Ledda · S. Tilocca
Department of Veterinary Medicine, of Sassari, Via Vienna 2,
07100 Sassari, Sardegna, Italy
e-mail: luis@uniss.it

M. Piccinini
ENEA C.R., Frascati, Rome, Italy

D. F. Albertini
Department of Molecular and Integrative Physiology, University of
Kansas Medical Center, Kansas City, KS, USA

exposure to cryoprotectants and the cold temperatures may lead to the disruption of microtubules and the change of the meiotic spindle morphology of mature oocytes [11–16]. Few reports focus on modifications caused by vitrification on the actin cytoskeleton [13, 17–21]. Actin is a major component of the cytoskeleton of the oocyte and it is present as the fibrous polymer, F-actin, in dynamic equilibrium with monomeric globular actin (G-actin). The mature oocyte presents at least two F-actin compartments, each with a distinct dynamic and regulation: the cortical F-actin which is localized into a uniform layer all around the oocyte cortex, and the cytoplasmic F-actin. Most development events, such as spindle positioning, polar body release, pronuclear migration and embryo cleavage are dependent on a well-defined dynamic and organization of the F-actin network. [9, 10].

Different methods have been used to study the proteins of the cytoskeleton in the oocyte, [22], but they often require cell fixation and specific labels [18, 23]. Recently, advances in imaging technology, as the polarized light microscopy technology, have offered the opportunity to visualize the meiotic spindle non-invasively before and/or after cryopreservation [24, 25]. The development of other approaches could facilitate the assessment of the changes caused by vitrification/warming on the cytoskeleton of the oocyte.

Raman microspectroscopy (RMS) is a physicochemical fingerprinting technique which is based on the inelastic scattering of laser photons by vibrating molecules found in the sample [26]. The analysis of scattered frequencies provides chemical and structural information which is characteristic of the molecules present in the sample. Raman offers the advantage of acquiring information regarding the biochemical constituents of the sample and their spatial distribution without labelling, on both fixed and unfixed cells. This technique has been, widely, used to study the biological changes of various cellular components during cell cycle progression, apoptosis, and response to stress [27]. On the other hand, studies focused on female gamete are restricted to a few works [28–32]. Specifically, changes of the molecular architecture of the oocyte at different maturation stages have been revealed by RMS [28–30]. Recently, our group demonstrated that RMS is able to assess the structural modifications of the zona pellucida of ovine oocytes following vitrification/warming [31]. Furthermore, the detection of chemical alterations caused by aging-related oxidative damage has been analyzed in mouse oocytes [32].

As an extension of our previous researches [31, 32], in this work we investigated the feasibility of RMS to identify changes occurring in the cortical F-actin network of in vitro matured ovine oocytes following exposure to cryoprotectants and vitrification. Moreover, immunofluorescence imaging of the cortical F-actin was performed by confocal microscopy on the same oocytes after completion of the RMS analysis.

Materials and methods

Collection and in vitro maturation of ovine oocytes

Cumulus–oocyte complexes (COCs) were recovered from the ovaries of slaughtered sheep (Sarda sheep, 4–6 years old). Only COCs showing several intact cumulus cell layers and uniform cytoplasm with homogeneously distributed lipid droplets were selected for in vitro maturation (IVM) in TCM 199 supplemented with 10 % (v/v) heat-treated estrus sheep serum (ESS), 0.1 IU/ml FSH, 0.1 IU/ml LH and 100 μ M cysteamine for 22 h in 5 % CO₂ in air at 38.5 °C. At the end of maturation, oocytes were completely denuded from cumulus cells by incubation with hyaluronidase. The assessment of nuclear maturation (MII stage) was performed by visualizing the presence of a polar body by a stereomicroscope (Olympus ZX40) at 40X magnification.

A group of MII oocytes was incubated with latrunculin-A (LATA) as described below. Another group was processed according to the experimental design. All the in vitro matured oocytes employed for the experiments derived from the same batches of ovaries.

Treatment with Latrunculin-A

Since the Raman spectrum of the oocyte cortex is, inherently, complex due to contribution of protein and lipid molecular vibrations, we, first, conducted studies to identify the regions of Raman spectrum representative of F-actin. Accordingly, the F-actin network was depolymerized in a group of MII oocytes ($n=10$, LATA) by incubation for 4 h (5 % CO₂ in air at 38.5 °C) in IVM medium containing 200 μ M Latrunculin-A (LATA). LATA is a widely employed, highly specific, and reversible F-actin depolymerizing agent, based on its stoichiometric binding with G-actin [33, 34]. A group of not-treated MII oocytes was used as control ($n=10$, CTR). CTR and LATA oocytes were processed for RMS measurements and data analyzed to identify spectral differences between the two groups. To evaluate the efficiency of LATA treatment to destabilize F-actin network, immuno-fluorescence imaging of F-actin was performed on the same oocytes after Raman analysis as detailed below.

Experimental design

In vitro matured oocytes were divided into three experimental groups:

- (1) Oocytes exposed to cry protectants ($n=10$, CPA-expr): submitted to all the vitrification/warming procedures excluding the plunge into liquid nitrogen.
- (2) Vitrified oocytes ($n=10$, VITRI).
- (3) Control oocytes ($n=10$, CTR): untreated oocytes.

Vitrification and warming

Vitrification was performed following the Minimum Essential Volume (MEV) method using the cryotop device [35]. Groups of five MII oocytes were equilibrated at 38.5 °C for 1 min in holding medium (HM) consisting of 20 mM Hepes-buffered TCM 199 supplemented with 20 % (v/v) fetal calf serum (FCS). After equilibration, oocytes were incubated in 10 % (v/v) ethylene glycol (EG) +10 % (v/v) dimethylsulfoxide (Me₂SO₄) in HM for 30 s and then transferred to 20 % (v/v) EG and 20 % (v/v) Me₂SO₄ and 0.5 M sucrose in HM for 20 s. They were, thereafter, loaded onto the cryotop, and immediately plunged into liquid nitrogen (LN₂) for cooling and storage. For warming, cryotops were directly immersed into HM supplemented with 1.25 M sucrose for 1 min at 38.5 °C. Oocytes were transferred into HM containing decreasing sucrose concentrations (0.62 and 0.31 M), and then washed in HM. Warmed oocytes were cultured for 1 h in TCM 199 supplemented with 10 % (v/v) ESS and processed for RMS measurement.

Preparation of oocytes for RMS analysis

All oocytes were fixed for 30 min in 4 % paraformaldehyde (w/v, PFA) solution. Fixation with PFA was used, as our preliminary experiments (data not shown) and the results of Davidson et al. [29] indicated that, PFA- fixed and unfixed oocytes showed similar results following Raman analysis compared to other fixative methods which caused modification of the spectra. After fixation, samples were washed in PBS and stored at 4 °C until RMS examination. For RMS analysis, each oocyte was immersed in a 100 µL drop of PBS overlaid with mineral oil on a quartz window.

Measurement by RMS

Measurements were performed using a Bruker Senterra confocal Raman microscope using a 532 nm excitation laser (wavelength) operated at 25 mW with spectra collected through a 60x water-immersion objective (numerical aperture: 1.1; working distance: 1.5 mm).

Data recording was performed by circumferential and sequential laser focusing at 12 points in the oocyte cortex just below the plasma membrane (Fig. 1a). The final spectrum recorded from each point was obtained averaging 6 acquisitions of 3 s at 9–15 cm⁻¹ resolution. Finally, the spectrum of each oocyte was calculated averaging the 12 spectra acquired along the subcortical region (approximately 3.5 min. acquisition time).

A chemical map of one quadrant of single CTR, CPA-exp VITRI oocytes was generated within a 70 by 70 µm grid (Fig. 1b). Individual spectra were obtained by averaging five acquisitions with duration of 5 s/scan. At this temporal

resolution, data acquisition required about 5 h. Only a portion of each oocyte was mapped to reduce the acquisition time for imaging an entire oocyte (about 20 h) in order to minimize X, Y-axis displacements during these protracted periods of data acquisition.

Immuno-fluorescence labeling and analysis by confocal microscopy

Immuno-fluorescence imaging of F-actin was performed on the same oocytes after completion of the Raman measurements. Oocytes were permeabilized using 0.1 % Triton X-100. F-actin was stained using Phalloidin (diluted 1/150, Invitrogen, Carlsbad, CA), DNA were counter-stained with of 4', 6-diamidino-2-phenylindole (DAPI, Sigma-Aldrich; 100 ng/ml). Images of F-actin were acquired by a confocal laser-scanning fluorescence microscope (Leica TCS SP5), equipped with 543 nm HeNe, 488 nm Argon and 405 nm 405-diode lasers using an oil immersion 40x objective (NA= 1,25) and recorded on a host computer. Oocytes were scanned through the Z-axis and the images of the F-actin were recorded on the section corresponding to the equatorial plane of the cell.

The cortical F-actin band was classified as: a) normal: an evenly stained layer of F-actin band immediately beneath the plasma membrane; b) abnormal: irregular, discontinuous or absent staining of F-actin band.

Data analysis

To investigate spectral changes between the experimental groups, principal component analysis (PCA) was performed in the 1800–600 cm⁻¹ spectral range. A 17-point smoothing was applied to all averaged spectra, the second derivative was calculated and PCA was applied to the second derivative spectra. Data were shown through score plots, in which every spectrum was represented as a single point in a multivariate space. Loading plots were used to assign coefficient to the relevant principal components. The OPUS-Quant package of the Bruker OPUS 6.5 software was used for statistical analysis.

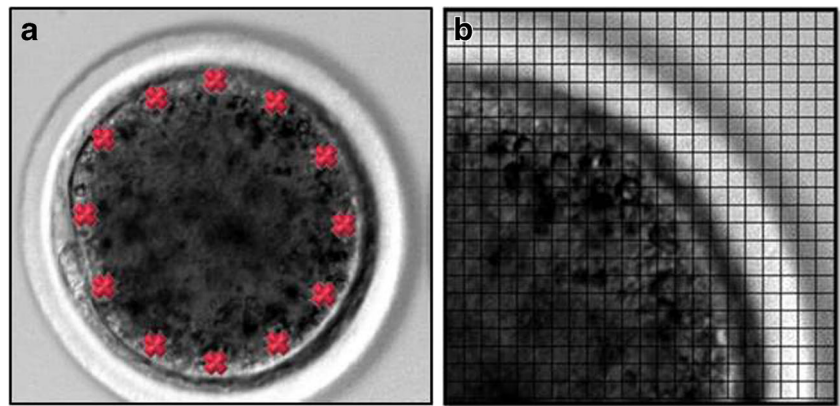
False color images were generated from each oocyte by integrating the Raman peaks under the spectral regions at 1657 cm⁻¹ (Amide I) and 1266–1300 cm⁻¹ (Amide III).

Results

Treatment with LATA

Figure 2a shows the average Raman spectra of CTR and LATA oocytes in the 1800–600 cm⁻¹ spectral range obtained after point scan measurements. It is possible to identify prominent spectral peaks in characteristic spectral regions. These

Fig. 1 Definition of RMS measurement by (a) point scans in the cortex of the and by (b) definition of a grid to obtain the mapping of one quadrant of an oocyte



features arise from the molecular vibration of components of the oocyte cortex such as lipids and proteins [27]. The spectral regions around 1655 cm^{-1} and in the 1230 cm^{-1} , 1320 cm^{-1} range are from amide I and amide III, respectively, which are predominately, associated with protein bond vibrations. The band at 1448 cm^{-1} represents the CH_2 bending vibration and CH_3 deformation of the proteins and lipids.

The PCA was performed on a data matrix that contained the 20 average spectra collected from the two sample groups

($n_{\text{CTR}}=10$; $n_{\text{LATA}}=10$). The PCA scatter plots (Fig. 2b) evidenced a marked separation of the two groups. The nature of chemical variation between the two groups can be showed by examination of the PCA loading plots (Fig. 2c) which presented positive peaks in the region 1657 cm^{-1} (Amide I), 1440 , $1300\text{--}1266\text{ cm}^{-1}$ (Amide III).

The observed differences can be considered indicative of the changes of the cortical F-actin, since the oocytes have been treated with a specific F-actin destabilizing drug. Nevertheless,

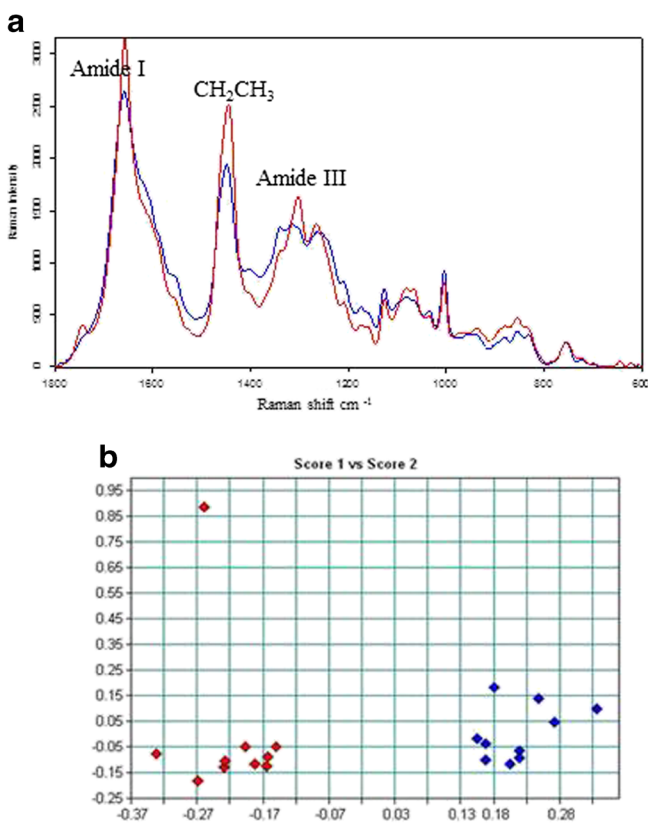
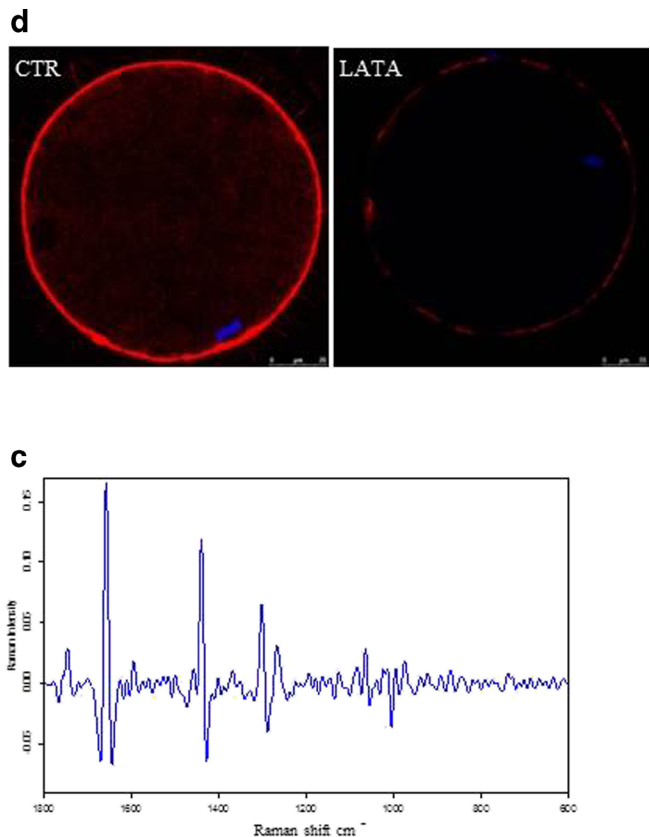


Fig. 2 a Average Raman spectra of CTR (red) and LATA (blue) oocytes in the $1800\text{--}600\text{ cm}^{-1}$ spectral range obtained after point scan measurements; b PCA score plot (PC1 vs PC2) and c PCA loading plot (PC2) applied to the second derivative of the two experimental classes. d



Immunostaining of cortical F-actin: normal F-actin distribution of in vitro matured oocyte (CTR) and low staining intensity and discontinuous distribution after LATA treatment (LATA)

it cannot be excluded that the destabilization of F-actin may have affected other components of the oocyte cortex, which could also contribute to the observed differences assessed by RMS.

Immuno-fluorescence images of F-actin showed an abnormal distribution of cortical F-actin (very low staining intensity) in all the oocytes treated with LATA, whereas CTR oocytes exhibited a compact and homogeneous bright staining pattern located in the oolemma periphery (Fig. 2d).

Exposure to cryoprotectants and vitrification

Figure 3a shows the average Raman spectra of CTR, CPA-exp and VITRI oocytes in the 1800–600 cm^{-1} spectral range obtained after point scan measurements.

The PCA was performed on a data matrix that contained the 30 average spectra collected from the three sample groups ($n_{\text{CTR}}=10$; $n_{\text{CPA-exp}}=10$; $n_{\text{VITRI}}=10$). The PCA score plots (Fig. 3b) showed a marked discrimination between CTR oocytes and CPA-exp/ VITRI groups. No distinctions existed between CPA-exp and VITRI Raman fingerprints. The main differences highlighted by PCA loadings (Fig. 3c) are referable to proteins (1657, 1440, 1300 cm^{-1}). Since F-actin is a major protein of the oocytes cortex and based on the results of LATA experiments, these differences may also be indicative of the changes of the cortical F-actin network.

Immuno-fluorescence staining of the cortical F-actin revealed an abnormal pattern of F-actin organization (irregular or discontinuous staining, Fig. 3d, panels b,c,) in all CPA-exp and VITRI oocytes, while CTR oocytes exhibited a normal and uniform organization of F-actin layer (Fig. 3d, panel a). The immunofluorescence findings were in agreement with the Raman results.

Raman spectral maps and immune-fluorescence imaging of F-actin

Optical, immunofluorescence (F-actin) and Raman spectral images of one quadrant of CTR, CPA-exp and VITRI oocytes are presented in Fig. 4. Univariate intensity maps have been constructed by integrating the Raman spectral region corresponding to Amide I (Fig. 4, Panel g,h,i) and Amide III (Fig. 4, Panel l,m,n). As such, these figures are indicative of the protein distribution within each of the sample. It can be, clearly, observed a high protein concentration in the cortex of the oocytes, just beneath the oolemma, although proteins are distributed through the cytoplasm. Moreover, the Raman chemical maps indicated that the protein distribution was altered in CPA-exp and VITRI oocytes (Fig. 4, Panel h,m,n) compared to CTR oocytes (Fig. 4, Panel g, l).

The immunofluorescence images of the cortical F-actin (Fig. 4, Panel d, e, f) showed that in CPA-exp and VITRI

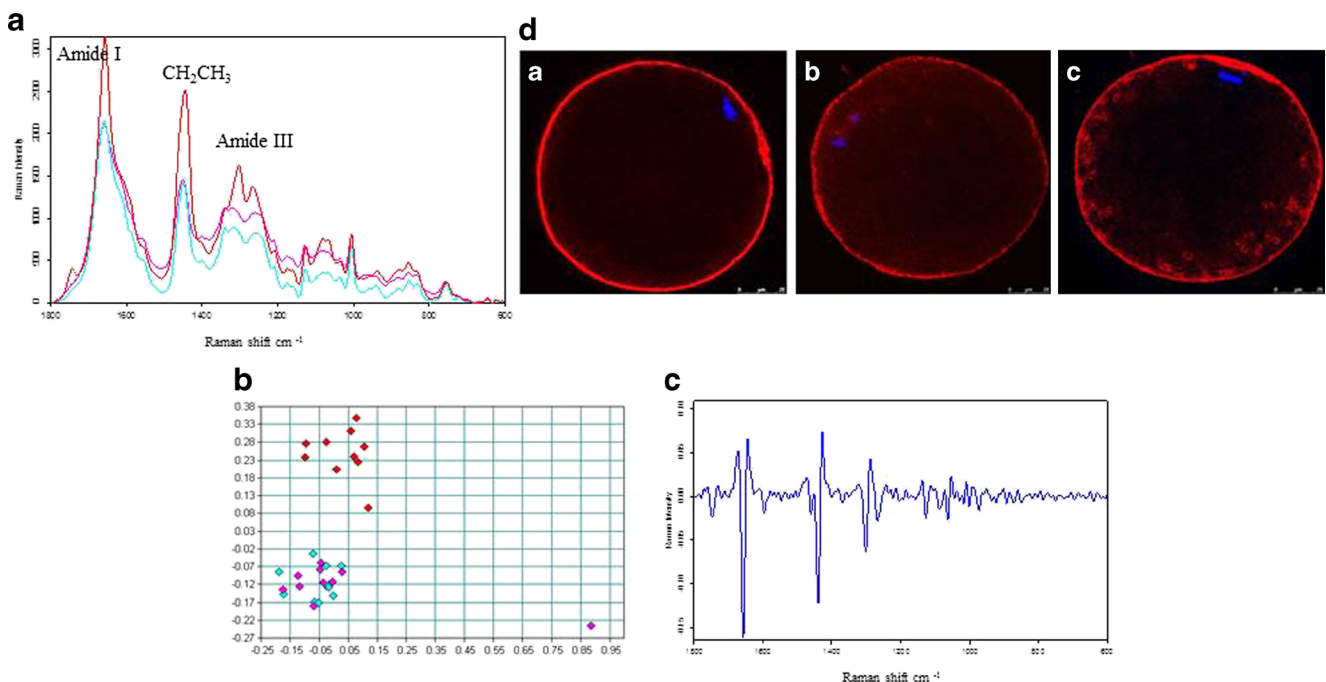


Fig. 3 a Average Raman spectra of CTR (red) and CPA-exp (pink), VITRI (blue) oocytes in the 1800–600 cm^{-1} spectral range obtained after point scan measurements; b PCA score plot (PC1 vs PC2) and c PCA loading plot (PC2) applied to the second derivative of the two experimental classes. Each dot represents the average spectrum of each oocyte;

d Immunostaining of F-actin: a normal homogeneous cortical actin network immediately beneath the plasma membrane (a) in contrast to a discontinuous and reduced (b) or an irregular and spotted (c) pattern of distribution of microfilaments in the cortical area

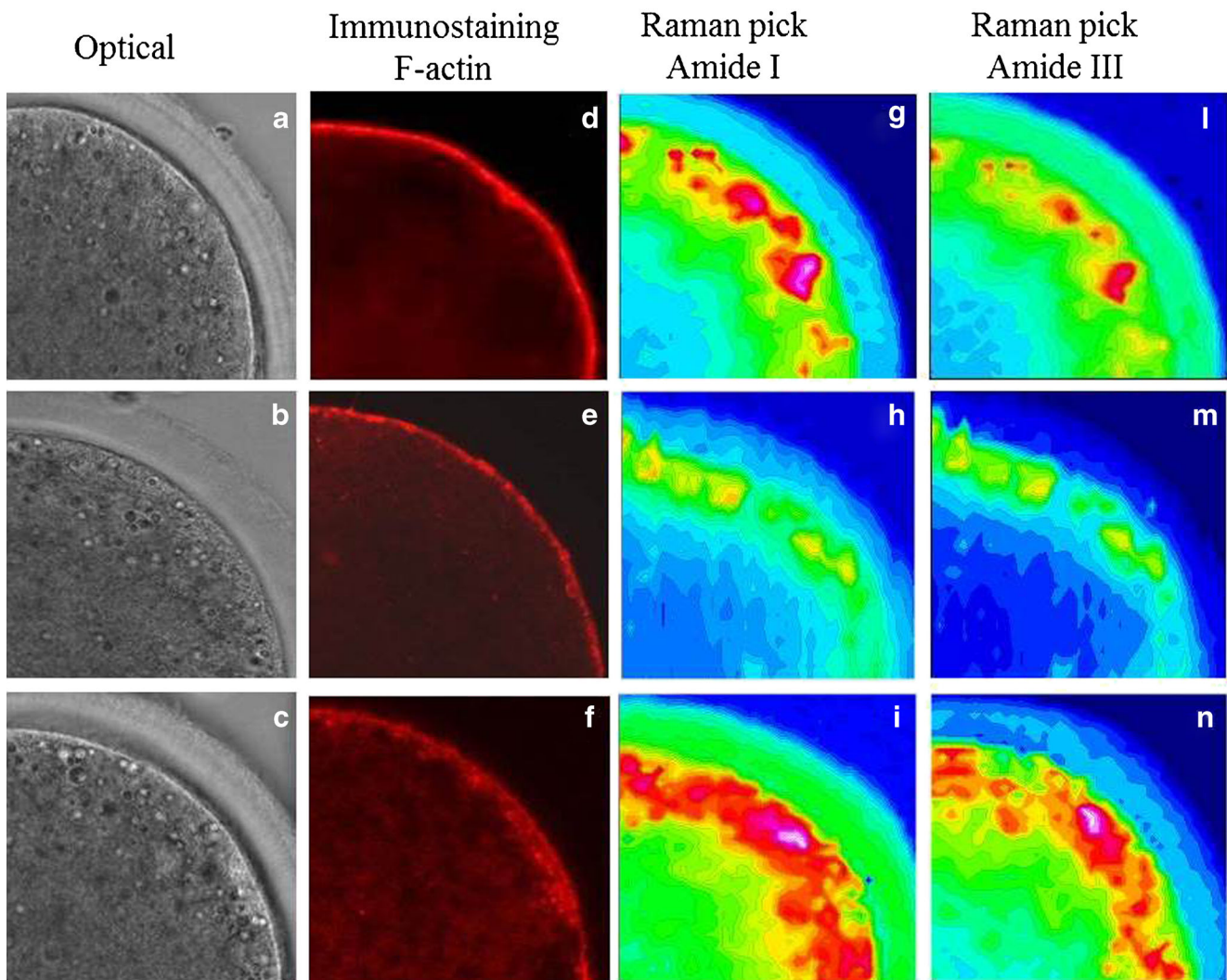


Fig. 4 Image panel displaying optical images (*a, b, c*), immunostaining of normal (*d*) and abnormal cortical F-actin (*e, f*) and the respective univariate Raman maps constructed by the intensity of Amide I (*g, h, i*) and Amide III (*l, m, n*) regions

oocytes there was an abnormal cortical F-cortical network respect to CTR oocytes which displayed a regular cortical F-actin band.

Discussion

The present study aimed to evaluate the feasibility of a label-free Raman microspectroscopy approach for visualizing the biochemical changes of proteins in the oocyte cortex following vitrification, with particular reference to the cortical F-actin. This purpose was motivated from the results of our previous study that demonstrated the potential use of this technique to detect modifications of the zona pellucida of cryopreserved in vitro matured ovine oocytes [31]. The power of this technique for the examination of the oocyte has been reported by the pivotal study of Wood et al. [28] which was

addressed to investigate the difference in the molecular architecture of immature and mature mouse oocytes. Later studies focused on the biochemical variation within oocytes and embryos at different stage of development [29, 30] and on the aging-related oxidative damage of mouse oocytes [32].

The findings of the present study add a new element on the application of RMS for the study of the oocyte. Specifically, analysis of the average spectra obtained after point scan measurement by PCA and Raman spectral maps provided an insight into the modifications induced by cryoprotectants and cold temperatures on the protein organization of the oocyte cortex. Such changes may likely include the modification of the cortical F-actin network. This assumption is derived from the Raman results obtained after treatment of MII oocytes with a specific F-actin destabilizing drug and it's also supported by the evidence that F-actin is a major component of oocyte cortex. Moreover, the good correspondence between results of PCA, Raman spectral images of proteins and the

immuno-fluorescence images of F-actin further support that actin is one of the main contributors to the measured Raman band of proteins. Similar comparisons between Raman spectral images and fluorescence images have been described for Raman label-free imaging of dendritic cells [36] and mitochondria [37].

In the present study, the Raman false color images of one quadrant of single oocytes revealed high protein intensities in the cortical region of the ooplasm. This distribution is consistent with the localization in the periphery of the mature oocytes of organelles, cortical granules and the presence of a thick F-actin band.

The Raman spectral data of proteins and the immunofluorescence images of F-actin indicated that exposure of in vitro matured ovine oocytes to concentration of DMSO and EG ranging from 10 % (equilibration solution) to 20 % (vitrification solution), seriously, altered the protein distribution of the oocyte cortex and also caused a severe disruption of the cortical F-actin network. We, previously, demonstrated [31] that the exposure of in vitro matured ovine oocytes to DMSO and EG, at the same concentration used in the present study, did not alter the secondary structure of protein and carbohydrate residues of the zona pellucida and affected the destabilization of the tubulin cytoskeleton in about 30 % of MII oocytes (unpublished data). Thus the cortical F-actin, in the ovine species, appeared more sensitive to such concentrations of DMSO and EG than other oocyte components.

The debate on how vitrification procedures affect the microfilament network of the immature or mature oocytes has been reported in several studies [8, 13, 17–21, 38–40]. Consequences of vitrification/warming on the actin cytoskeleton depended on the CPAs used, the oocyte maturation stage and varied between species. In the ovine species investigations on the modification of microfilaments during vitrification of the mature oocyte are currently lacking.

The actin cytoskeleton, in mammalian oocytes, is a dynamic system that directs a number of events during oocyte maturation and fertilization such as the establishment of oocyte polarity, spindle anchoring and orientation, pronuclear migration and embryo development. F-actin, also, plays an important role in the distribution of some organelles as Golgi complex and mitochondria, ion channel regulation and the spatial positioning of mRNA [9, 10]. Pharmacological treatments that disrupt the actin cytoskeleton, adversely, affect mouse fertilization and early embryo division [41] and the inhibition of F-actin polymerization prevents completion of meiosis and embryo development in pig oocytes [42].

In order to protect microfilaments from the negative effects of CPAs, drugs which reversibly depolymerized the F-actin network has been used prior to freezing of mature mouse oocytes [43]. These oocytes resulted in high post thaw survival and, significantly, improved developmental competence

[38]. Moreover, a protective effect of antifreeze protein 3 on the cortical F-actin of vitrified/warmed mature mouse oocytes has been reported [44].

Until recently, the study of the role of actin and its dynamic was focused, mostly, on the contribution of the cortical F-actin, using the fluorescently labeled phalloidin [45] which strongly stains the cortex. However during the last years, the development of new actin probes that bind to F-actin rather than G-actin, such as Lifeact or GFP-UtrCh revealed other pools of F-actin in the cytoplasm or around the spindle in mitotic cells [46]. Recently, the use of this probe coupled with live imaging and biophysical approach resulted in new relevant discoveries [47]. In particular, this research revealed new levels of complexity in the dynamic and regulation of F-actin during meiotic maturation of mouse oocytes and linked the thickening of the cortical F-actin (composed by two distinct outer and inner layers) to an increase in cortical plasticity.

In our preliminary study, RMS has been employed to evaluate the alteration of proteins and, among them, the F-actin in the oocyte cortex without considering the behavior of other actin pools or the different dynamic of F-actin in different regions of the oocyte cortex or in the cytoplasm.

Further studies and technical improvements are needed to expand the applicative potentiality of RMS as useful tool for proper assessment of the oocyte. Certainly, it is imperative, for the application in live cells, to reduce the time required for spectral acquisition. To overcome this limitation a point scans measurements [present work, 31] and line scans measurements [32] can be used. The use of resonant Raman excitation such as coherent anti-Stokes Raman scattering microscopy (CARS) can, also, speed the Raman data acquisition [48]. Furthermore, the use of controlled condition during (e.g. temperature, sterile/single-use supports, appropriate holding medium) are required to implement the safety of RMS during the analysis of the oocyte. Finally, the contribution of multi-disciplinary experts could help for a careful interpretation and a strict validation of the results.

References

1. Konc J, Kanyó K, Kriston R, Somoskői B, Cseh S. Cryopreservation of embryos and oocytes in human assisted reproduction. *Biomed Res Int.* 2014;2014:307268.
2. Saragusty J, Arav A. Current progress in oocyte and embryo cryopreservation by slow freezing and vitrification. *Reproduction.* 2011;141:1–19.
3. Mullen SF, Fahy GM. A chronologic review of mature oocyte vitrification research in cattle, pigs, and sheep. *Theriogenology.* 2012;78:1709–19.
4. The Practice Committees of the American Society for Reproductive Medicine and the Society for Assisted Reproductive Technology. Mature oocyte cryopreservation: a guideline. *Fertil Steril.* 2013;99:37–43.

5. Arav A, Natan Y. Vitrification of oocytes: from basic science to clinical application. *Adv Exp Med Biol*. 2013;761:69–83.
6. Diez C, Muñoz M, Caamaño JN, Gómez E. Cryopreservation of the bovine oocyte: current status and perspectives. *Reprod Domest Anim*. 2012;3:76–83.
7. Vincent C, Johnson MH. Cooling, cryoprotectants, and the cytoskeleton of the mammalian oocyte. *Oxf Rev Reprod Biol*. 1992;14:73–100.
8. Moussa M, Shu J, Zhang X, Zeng F. Cryopreservation of mammalian oocytes and embryos: current problems and future perspectives. *Sci China Life Sci*. 2014;57:903–14.
9. Li R, Albertini DF. The road to maturation: somatic cell interaction and self-organization of the mammalian oocyte. *Nat Rev Mol Cell Biol*. 2013;14:141–52.
10. Simerly C, Navara CS, Wu GJ, Schatten G. Cytoskeletal organization and dynamics in mammalian oocytes during maturation and fertilization. In: Grudzinskas JG, Yovich JL, editors. *Gametes - the oocyte*. Cambridge: Cambridge University Press; 1995. p. 54–94.
11. Lei T, Guo N, Liu JQ, Tan MH, Li YF. Vitrification of in vitro matured oocytes: effects on meiotic spindle configuration and mitochondrial function. *Int J Clin Exp Pathol*. 2014;7:1159–65.
12. Tamura AN, Huang TT, Marikawa Y. Impact of vitrification on the meiotic spindle and components of the microtubule-organizing center in mouse mature oocytes. *Biol Reprod*. 2013;89:112.
13. Egerszegi I, Somfai T, Nakai M, Tanihara F, Noguchi J, Kaneko H, et al. Comparison of cytoskeletal integrity, fertilization and developmental competence of oocytes vitrified before or after in vitro maturation in a porcine model. *Cryobiology*. 2013;67:287–92.
14. Coticchio G, Bromfield JJ, Sciajno R, Gambardella A, Scaravelli G, Borini A, et al. Vitrification may increase the rate of chromosome misalignment in the metaphase II spindle of human mature oocytes. *Reprod Biomed Online*. 2009;19:29–34.
15. Chen SU, Yang YS. Slow freezing or vitrification of oocytes: their effects on survival and meiotic spindles, and the time schedule for clinical practice. *Taiwan J Obstet Gynecol*. 2009;48:15–22.
16. Succu S, Leoni GG, Bebbere D, Berlinguer F, Mossa F, Bogliolo L, et al. Vitrification devices affect structural and molecular status of in vitro matured ovine oocytes. *Mol Reprod Dev*. 2007;74:1337–44.
17. Mikołajewska N, Müller K, Nizański W, Jewgenow K. Vitrification of domestic cat oocytes—effect on viability and integrity of subcellular structures. *Reprod Domest Anim*. 2012;47:295–9.
18. Wu C, Rui R, Dai J, Zhang C, Ju S, Xie B, et al. Effects of cryopreservation on the developmental competence, ultrastructure and cytoskeletal structure of porcine oocytes. *Mol Reprod Dev*. 2006;73:1454–62.
19. Rojas C, Palomo MJ, Albarracín JL, Mogas T. Vitrification of immature and in vitro matured pig oocytes: study of distribution of chromosomes, microtubules, and actin microfilaments. *Cryobiology*. 2004;49:211–20.
20. Hotamisligil S, Toner M, Powers RD. Changes in membrane integrity, cytoskeletal structure, and developmental potential of murine oocytes after vitrification in ethylene glycol. *Biol Reprod*. 1996;55:161–8.
21. Combelles CM, Ceyhan ST, Wang H, Racowsky C. Maturation outcomes are improved following Cryoleaf vitrification of immature human oocytes when compared to choline-based slow-freezing. *J Assist Reprod Genet*. 2011;28:1183–92.
22. Azoury J, Lee KW, Georget V, Hikal P, Verlhac MH. Symmetry breaking in mouse oocytes requires transient F-actin meshwork destabilization. *Development*. 2011;138:2903–8.
23. Khalili MA, Maione M, Palmerini MG, Bianchi S, Macchiarelli G, Nottola SA. Ultrastructure of human mature oocytes after vitrification. *Eur J Histochem*. 2012;56:e38.
24. Caamaño JN, Muñoz M, Diez C, Gómez E. Polarized light microscopy in mammalian oocytes. *Reprod Domest Anim*. 2010;2:49–56.
25. Coticchio G, Sciajno R, Hutt K, Bromfield J, Borini A, Albertini DF. Comparative analysis of the metaphase II spindle of human oocytes through polarized light and high-performance confocal microscopy. *Fertil Steril*. 2010;93:2056–64.
26. Nottinger I, Hench LL. Raman microspectroscopy: a noninvasive tool for studies of individual living cells in vitro. *Expert Rev Med Devices*. 2006;3:215–34.
27. Matthaus C, Bird B, Miljkovic M, Chemenko T, Romeo M, Diem M. Infrared and Raman microscopy in cell biology. *Methods Cell Biol*. 2008;89:275–308.
28. Wood BR, Chemenko T, Matthaus C, Diem M, Chong C, Bernhard U, et al. Shedding new light on the molecular architecture of oocytes using a combination of synchrotron fourier transm-infrared and Raman spectroscopic mapping. *Anal Chem*. 2008;80:9065–72.
29. Davidson B, Murray AA, Elfick A, Spears N. Raman microspectroscopy can be used to investigate the developmental stage of the mouse oocyte. *PLoS One*. 2013;8:e67972.
30. Davidson B, Spears N, Murray A, Elfick A. The changing biochemical composition and organisation of the murine oocyte and early embryo as revealed by Raman spectroscopic mapping. *J Raman Spectrosc*. 2012;43:24–31.
31. Bogliolo L, Ledda S, Innocenzi P, Ariu F, Bebbere D, Rosati I, et al. Raman microspectroscopy as a non-invasive tool to assess the vitrification-induced changes of ovine oocyte zona pellucida. *Cryobiology*. 2012;64:267–72.
32. Bogliolo L, Murrone O, Di Emidio G, Piccinini M, Ariu F, Ledda S, et al. Raman spectroscopy-based approach to detect aging-related oxidative damage in the mouse oocyte. *J Assist Reprod Genet*. 2013;30:877–82.
33. Spector I, Shochet NR, Blasberger D, Kashman Y. Latrunculins—novel marine macrolides that disrupt microfilament organization and affect cell growth: I. Comparison with cytochalasin D. *Cell Motil Cytoskeleton*. 1989;13:127–44.
34. Spector I, Shochet NR, Kashman Y, Groweiss A. Latrunculins: novel marine toxins that disrupt microfilament organization in cultured cells. *Science*. 1983;219:493–5.
35. Kuwayama M, Vajta G, Kato O, Leibo SP. Highly efficient vitrification method for cryopreservation of human oocytes. *Reprod BioMed Online*. 2005;11:300–8.
36. Zoladek AB, Johal RK, Garcia-Nieto S, Pascut F, Shakesheff KM, Ghaemmaghami AM. Nottinger Label-free molecular imaging of immunological synapses between dendritic and T cells by Raman micro-spectroscopy. *Analyst*. 2010;135:3205–12.
37. Matthäus C, Chernenko T, Newmark JA, Warner CM, Diem M. Label-free detection of mitochondrial distribution in cells by nonresonant Raman microspectroscopy. *Biophys J*. 2007;93:668–73.
38. Kim SS, Olsen R, Kim DD, Albertini DF. The impact of vitrification on immature oocyte cell cycle and cytoskeletal integrity in a rat model. *J Assist Reprod Genet*. 2014;31:739–47.
39. Albarracín JL, Morató R, Rojas C, Mogas T. Effects of vitrification in open pulled straws on the cytology of in vitro matured prepubertal and adult bovine oocytes. *Theriogenology*. 2005;63:890–901.
40. Lee K, Wang C, Spate L, Murphy CN, Prather RS, Machaty Z. Gynogenetic activation of porcine oocytes. *Cell Reprogram*. 2014;16:121–9.
41. Maro B, Johnson MH, Pickering SJ, Flach G. Changes in actin distribution during fertilization of the mouse egg. *J Embryol Exp Morphol*. 1984;81:211–37.
42. Lee K, Wang C, Spate L, Murphy CN, Prather RS, Machaty Z. Gynogenetic activation of porcine oocytes. *Cell Reprogram*. 2014;16:121–9.
43. Hosu BG, Mullen SF, Critser JK, Forgacs G. Reversible disassembly of the actin cytoskeleton improves the survival rate and developmental competence of cryopreserved mouse oocytes. *PLoS One*. 2008;30:3–e2787.
44. Wen Y, Zhao S, Chao L, Yu H, Song C, Shen Y, Chen H, Deng X. The protective role of antifreeze protein 3 on the structure and

- function of mature mouse oocytes in vitrification. *Cryobiology*. 2014, in press.
45. Cooper JA. Effects of cytochalasin and phalloidin on actin. *J Cell Biol*. 1987;105:1473–8.
 46. Riedl J, Crevenna AH, Kessenbrock K, Yu JH, Neukirchen D, Bista M, et al. Lifeact: a versatile marker to visualize F-actin. *Nat Methods*. 2008;5:605–7.
 47. Chaigne A, Campillo C, Gov NS, Voituriez R, Azoury J, Umaña-Diaz C, et al. A soft cortex is essential for asymmetric spindle positioning in mouse oocytes. *Nat Cell Biol*. 2013;15: 958–66.
 48. Downes A, Mouras R, Bagnaninchi P, Elfick A. Raman spectroscopy and CARS microscopy of stem cells and their derivatives. *J Raman Spectrosc*. 2011;42:1864–70.